

# Millibot Trains for Enhanced Mobility

H. Benjamin Brown, Jr., J. Michael Vande Weghe, Curt A. Bererton, and Pradeep K. Khosla, *Fellow, IEEE*

**Abstract**—The objective of this work is to enhance the mobility of small mobile robots by enabling them to link into a train configuration capable of crossing relatively large obstacles. In particular, we are building on *Millibots*, semiautonomous, tracked mobile sensing/communication platforms at the 5-cm scale previously developed at Carnegie Mellon University. The *Millibot Train* concept provides couplers that allow the Millibot modules to engage/disengage under computer control and joint actuators that allow lifting of one module by another and control of the whole train shape in two dimensions. A manually configurable train prototype demonstrated the ability to climb standard stairs and vertical steps nearly half the train length. A fully functional module with powered joints has been developed and several have been built and tested. Construction of a set of six modules is well underway and will allow testing of the complete train in the near future. This paper focuses on the development, design, and construction of the electro-mechanical hardware for the Millibot Train.

**Index Terms**—Distributed robotics, mobility, modularity, snakes, trains.

## I. INTRODUCTION

RECENTLY there has been increasing interest in distributed robotic systems whereby tasks are executed not by single robots, but by teams of collaborating robots [1]–[4]. Team members may cooperate to explore unknown spaces, exchange sensor information, provide surveillance data, manipulate heavy objects, or carry out any of a number of tasks. Typically small in size, such robots can be maneuverable in tight areas and well-suited for covert activities. Individual robot modules may be endowed with specialized sensing, processing, mobility or manipulation capabilities to complement those of other team members. The distributed nature of the group may provide the team with redundant capabilities and/or information storage so a single failure does not disable the entire team. Physically distributed, these robots can provide varied viewpoints for sensing and perception and broad coverage for task execution. Potential tasks include surveillance, monitoring, sample collection, demining, and chemical plume detection.

Manuscript received March 31, 2002; revised October 1, 2002. Recommended by Guest Editors W.-M. Shen and M. Yim. This work was supported by the Defense Advanced Research Projects Agency's (DARPA) Distributed Robotics Program under Grant DABT63-97-1-0003.

H. B. Brown, Jr. and C. A. Bererton are with the Robotics Institute, Carnegie Mellon University, Pittsburgh, PA 15213 USA (e-mail: hbb@ri.cmu.edu; curtb@andrew.cmu.edu).

J. M. Vande Weghe was with the Institute for Complex Engineered Systems (ICES), Carnegie Mellon University, Pittsburgh, PA 15213 USA. He is now with the Neurobotics Laboratory, Robotics Institute, Carnegie Mellon University, Pittsburgh, PA 15213 USA (e-mail: vandeweg@cmu.edu).

P. K. Khosla is with the Department of Electrical and Computer Engineering (ECE) Carnegie Mellon University, Pittsburgh, PA 15213 USA (e-mail: pkk@ece.cmu.edu).

Digital Object Identifier 10.1109/TMECH.2002.806226

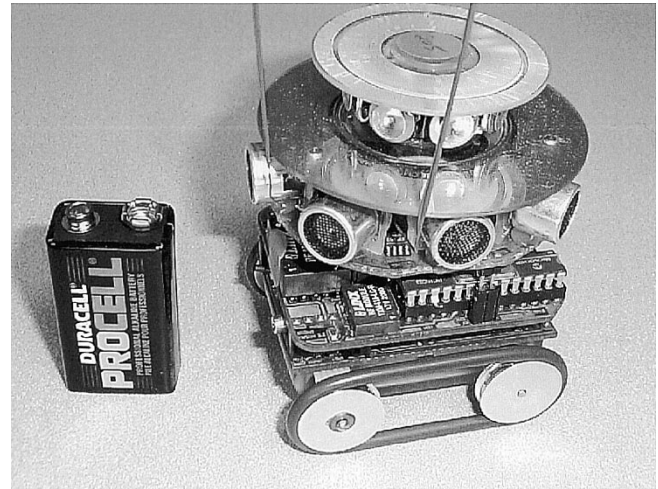


Fig. 1. Original Millibot, showing track base, sonar transmitters/receivers, and wireless communication.

Development of the Millibots has been underway for a number of years at Carnegie Mellon, with emphasis on sensors, communication capabilities and the high-level aspects of cooperative tasks [5], [6]. As shown in Fig. 1, a small mobile platform was developed, including: a skid-steered twin-track base, on-board battery power, an RF communication package, one or more sensing devices and a microprocessor for low-level control, sensor data processing and general coordination of activities. Each Millibot has a top speed of about 20 cm/s on smooth surfaces, a range of about 30–50 m on a battery charge, and nominally fits into a 5-cm cube. Typical sensors include: ultrasonics for obstacle detection and inter-module ranging up to a meter; IR sensors for short-range obstacle detection (< 10 cm range); a miniature CMOS video camera (0.8- $\mu$ m sensor) with transmitter; and pyro-electric sensors for detection of humans and other warm bodies.

The small size of the Millibots provides good maneuverability and allows them to operate inconspicuously, but places severe limitations on their mobility over rough terrain. Ideally, Millibots should be able to navigate normal outdoor terrains including grass, dirt, rocky areas, curbs and steps, as well as indoor environments. The goal of the present work is to enhance the mobility of the Millibots to allow them to operate in such areas. The work builds upon those who have created reconfigurable robot modules [7]–[13], snake-like robots [14]–[18], specialized stair-climbing robots [19]–[21] and trains of wheeled or tracked robots [22]–[25]. It has been shown that step-climbing and ditch-crossing ability are related to the wheel diameter (or front sprocket diameter for tracked vehicles), vehicle length and effective friction coefficients with the contact surfaces [26]. Especially on soft ground, tracked vehicles provide greater traction than wheeled vehicles [27].

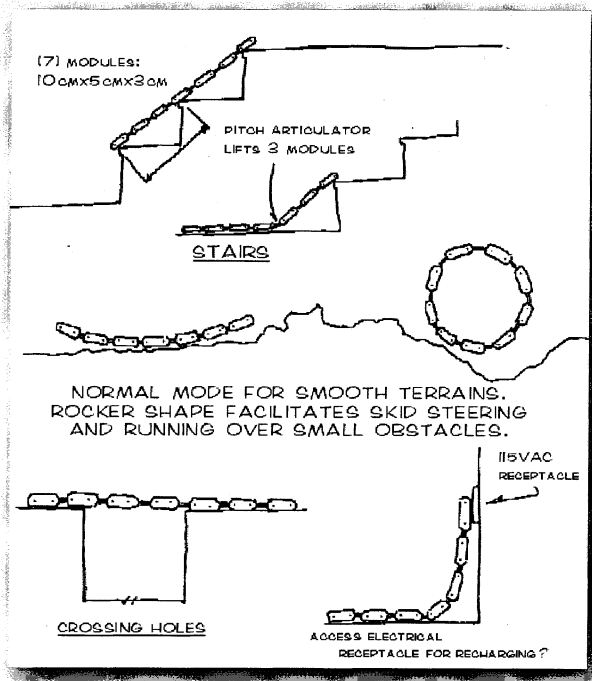


Fig. 2. Possible new modes of locomotion for a train of linked Millibots.

Based on such considerations, we developed the concept of the Millibot Train, wherein individual Millibot modules with powered tracks link into a train configuration to negotiate difficult terrain; then unlink and disperse to perform distributed activities. This paper focuses on the electro-mechanical design and construction of the Millibot Train.

## II. MILLIBOT TRAIN CONCEPT

Fig. 2 shows the basic capabilities envisioned for the Millibot Train. Powered links between the modules allow the train to conform to the terrain and adopt the desired shape for a particular task and to lift multiple modules to surmount obstacles. For example, the train can be locked into a straight shape for crossing ditches. A rocker shape is useful for traveling on flat or moderate terrain while facilitating skid-steering with the middle modules; in this configuration, the reduced contact length minimizes the resistance to yaw motion. For stair climbing, the articulation actuators lift the first few modules above the nose of the step. The train can then drive up the steps in a straight configuration, or a traveling wave shape can be adopted to better conform to the steps and reduce the traction needed. For climbing standard stairs, a minimum of seven modules (each approximately 10-cm long) is required to assure spanning at least two steps at all times. Cantilever lifting of three modules is needed to reach the nose of the first step. The concept includes movement in the sagittal plane but does not include lateral articulations, since they would add substantially to the size, weight, and complexity of the modules without greatly improving obstacle-crossing ability.

The original Millibot Train module concept is shown in Fig. 3. Wide, individually-powered caterpillar tracks provide drive traction and skid-steering ability. A two-pin coupler and

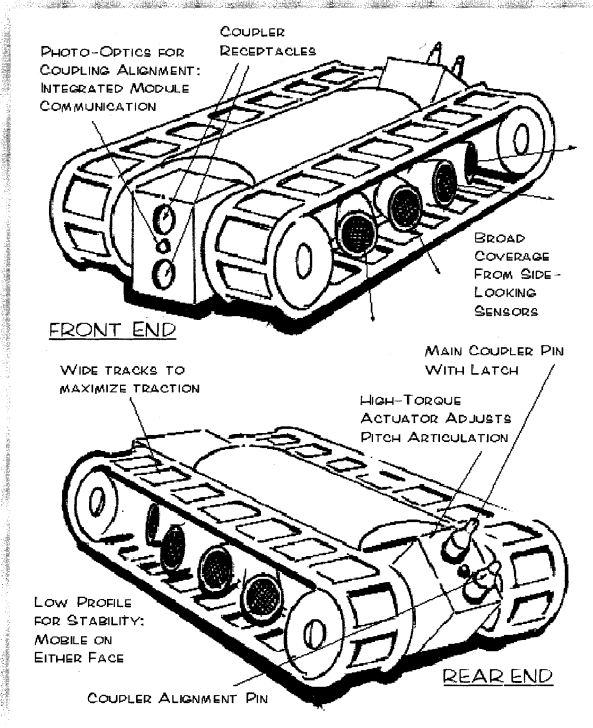


Fig. 3. Original concept of a Millibot Train module.

latch mechanism with a matching receptacle at the opposite end allows modules to drive together and dock with each other. A high-torque actuator drives the coupler articulation for lifting and holding modules in the desired configuration. The tracks cover most of the top and bottom and the surfaces between the tracks are smooth to minimize drag and the possibility of catching on terrain features. The tracks extend beyond the top and bottom faces allowing operation upside-down (and in fact, there is no preferred top or bottom.) Nominal dimensions of 3 cm high  $\times$  5 cm wide  $\times$  10 cm long were selected to conform approximately to the 5-cm cube specification in terms of module volume. This flat shape provides attitude stability and reduces the probability of a module (or the train) becoming stuck on its side.

This design requires creativity in locating the sensors used on the original Millibots. Sensors can be mounted to look out from inside the track loops similar to the ultrasonic sensors shown in the figure. Openings in the track could permit sensors to look upward/downward through the track, or possibly fore/aft through the sprockets. Sensors might be deployed from the top surface as needed, then retracted into the body for protection. Small sensors could be mounted on the coupler—where they could be tilted by the articulator for increased view—and on the receptacle at the other end. Another possibility is to have sensor modules that could be carried on the coupler: for example, the steering and lift mechanism could provide pan and tilt functions for a small camera latched onto the coupler. In previous work [28] we have designed two possible docking systems which may be integrated into this design to allow for autonomous coupling of the modules. However, the primary focus of this research is

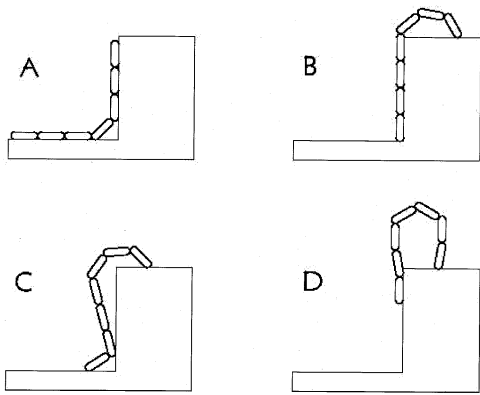


Fig. 4. Train of Millibots climbing a large step. (A) Forward modules being driven up the step by those still on the ground. (B) Topmost modules lifting and helping to hold the others against the face to maintain traction. (C) An alternate position may be assumed if the friction on the top surface is lower. (D) Once the last module nears the top the forward modules can bend and resume forward travel.

on mobility, so we will postpone most of the external sensing and high-level control issues for future work.

### III. MOBILITY CONSIDERATIONS

Quasi-static mobility<sup>1</sup> of surface vehicles depends basically on vehicle size, traction coefficients (friction) and overall configuration. The Millibot Train has great potential for mobility due to its relative length and ability to configure itself appropriately. With all couplers locked in a roughly straight pose, the train should be able to cross a ditch nearly half its length. A standard staircase step is easily crossed by lifting the front end of the train above the nose of the step, then following an S-curve to mount the step. The lifting capability is critical for steps with nose extensions that block directly climbing the vertical face (riser).

Higher steps, on the order of half the train length, require more finesse. As shown in Fig. 4(a), the front modules can be driven straight upward along the face of the step as long as the rear modules remaining on flat ground have enough power and traction to push. Simplistically, a train with passive joints can climb until the weight of the vertical modules is balanced by the traction forces against the wall. These traction forces depend on the forward thrust generated by the modules on the flat. The limit is  $N_v/N \leq \mu^2$ , where  $\mu$  is the friction coefficient (for both the horizontal and vertical surfaces),  $N$  is the total number of modules in the train, and  $N_v$  is the number of modules against the vertical face. Thus, for a typical friction coefficient of 0.7, half of the modules could be driven to vertical; a coefficient of 0.5 allows only one fourth to be lifted. However, the powered articulation of the Millibot train increases this lifting ability substantially by augmenting the lifting force applied to the vertical modules. In reality, the ability to balance the vertical column is likely to be the limiting factor.

Another limitation on step climbing is the ability to pull the train onto the plateau at the top of the step. The analysis is similar to the previous lifting analysis in that lateral thrust produces the normal force for traction against the wall. However, the robot

<sup>1</sup>“Quasi-static” means that only gravity, contact and traction forces are considered. Velocities are assumed small so that momentum effects are negligible.

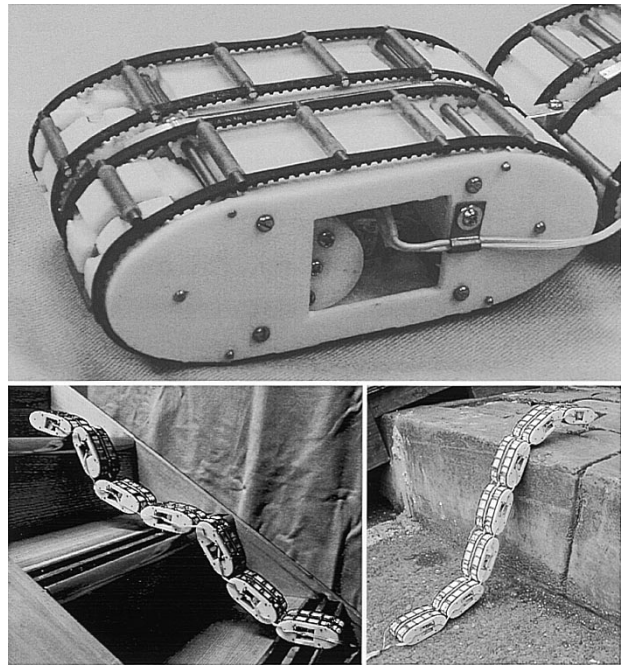


Fig. 5. Prototype used for testing train mobility. Top: detail of a single module, fabricated largely from FDM parts. Bottom: Seven modules climbing a standard flight of stairs (left) and a double-height step (right).

must curl around to contact the top surface [Fig. 4(b)], which places the contact point away from the nose of the step. Depending on the friction and geometric parameters, the robot may be unable to hold this pose and may be stable instead as shown in pose C.

As with the “pushing” case above, joint actuation can help to “pull” the robot above the nose of the step, gradually transferring load to the forward contact point [Fig. 4(d)], providing traction to drive forward. Clearly, strong joint actuation is critical for getting over the nose of the step.

### IV. MOBILITY TEST PROTOTYPE

In order to verify the mobility effectiveness of the train concept, a simple, manually-controlled, seven-module prototype was built as shown in Fig. 5. Each module includes a pair of small hobby servos independently driving the two tracks. The tracks were each formed from a pair of thin timing belts (3-mm wide, 2.03-mm pitch) connected by tubular cross bars glued to the belts. Thin rubber tubing over each cross bar provided a traction surface. Each belt was guided on an idler sprocket and a second sprocket driven by the hobby servo through a short timing belt. Modules were joined with friction couplers that would hold the manually set articulation angles. Overall length of the train was 0.75 m.

An interesting feature of this design was the extensive use of fused-deposition-modeling (FDM) rapid-prototyping for the manufacture of most of the parts. Parts were produced from P1500 polyester on a Stratasys Genisys FDM machine from ProEngineer<sup>2</sup> CAD models, to a resolution of 0.3 mm. Relatively complex parts, such as the hollow timing-belt sprockets

<sup>2</sup>ProEngineer is a registered trademark of Parametric Technology Corporation, Needham, MA 02494, USA.

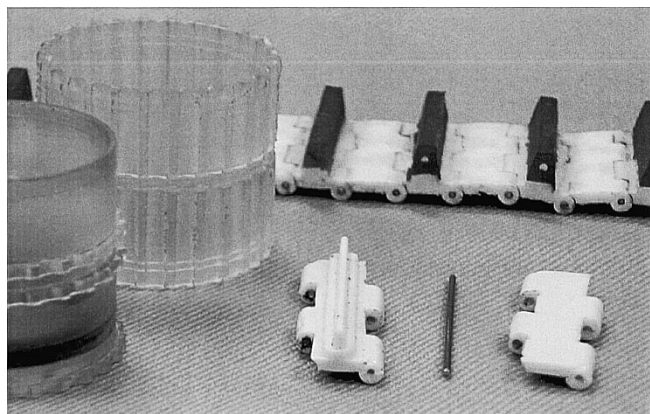


Fig. 6. Components of the module's track system, including the polycarbonate driving and idling sprockets (left), the individual track segments (right) and an assembled track with the polyurethane-covered growers (rear).

with internal ribs, could be easily and cheaply produced this way. FDM allowed substantial weight savings compared to conventional machining techniques and enabled quick, low-cost manufacturing of parts for the seven modules.

The train was wired to a manual switch box with battery pack, allowing ganged control of the left and right tracks. To emulate the performance of a train with powered articulations, we alternately drove the machine forward a short distance and manually adjusted the joint angles. With this method, the train was able to climb various standard staircases and even a step approximately 0.33-m high.

## V. MECHANICAL SYSTEMS

Once we had proven the concept of a two-sided, tracked vehicle in both individual and train configurations, we identified four major technical hurdles to achieve a fully functional system: tracks that would grip a variety of surfaces yet require minimal power to drive; a compact, efficient drive system to propel the two tracks; a coupling mechanism to allow the vehicles to join securely into the train configuration and then separate easily on command; and a strong, compact lifting mechanism to enable the train to change its shape.

### A. Tracks

Our goal for the tracks was to develop a profile that had large enough growers (the protrusions sticking out radially from tank-type treads) to engage the corners of stair treads, but that ran smoothly on flat surfaces. We wanted tracks that had low operating friction in order to maximize the available power and that were securely guided so that they would not be driven off of their sprockets even when subjected to large side forces. They also had to be relatively thin to preserve the vehicle's small size and wide enough to cover most of the vehicle's outer surface to reduce the chance of hang ups.

Although the tracks fabricated for the mobility-test prototype provided good traction on a variety of surfaces, the internal losses in bending the rubber timing belts consumed a large percentage of the available drive power. The final, low-loss design consisted of plastic track segments joined together with 0.8-mm steel pins (Fig. 6). Each segment was injection-molded

in-house from polycarbonate and alternate segments featured a thin growser onto which polyurethane rubber was cast. Each segment included a small transverse rib on the underside for lateral alignment. Each track was driven by a round sprocket cut with axial grooves to engage the track's hinge protrusions and cut with a circumferential groove to guide the underside rib.

The resulting design provided for much lower operating friction, high impact strength and very good traction, owing to both the growser shape and the sticky polyurethane covering. In achieving this performance, however, the possibility of sensors seeing through the track was lost. Manufacturing the track links was fairly straightforward, although we found that it was critical to control the mold temperature and flow rate to prevent nonuniform shrinkage and resultant residual stresses.

The polycarbonate track was tested by running it continuously at operating speed for two weeks while monitoring the current drawn by the driving motor as a measure of the track's operating friction. We found that the friction dropped steadily during a break-in period of 12 hours and then continued to run reliably without additional change. Some track segments showed early cracking and breakage of their hinge tabs, likely due to residual stresses from the molding process, but such failures usually occurred within the first six hours of run in, making it easy to separate out any defective segments from the final units.

### B. Drive

The two tracks are driven by small dc motors through a speed-reduction mechanism. The engineering challenge was to develop an efficient, compact, lightweight drive actuator with sufficient torque for the application. The worst-case design situation is when the train is climbing tangentially up a flight of stairs and the power to drive all seven modules is borne by just four drive units (left and right drives of the two modules that are touching stair noses). Based on a seven-module train and estimated module mass of 200 g, the target traction (thrust force) for each actuator was 1.8 N. To save precious space for batteries, sensors and electronics, we decided that the entire drive actuator for each track should fit inside the drive sprocket for that track. We had hoped to find a commercially-available motor/drive package that would meet our requirements, but soon discovered that available dc gearmotors of adequate power (from MicroMo, Smoovy, Maxon, etc.) were too long to fit the 2-mm axial space available. In the hobby market, we found the Mabuchi RF-020TH motor, which fit the space and provided reasonable torque, but left little axial space for gear reduction. Based on the available continuous motor torque (1.5 mN · m from our tests) and expected 75% drive train efficiency, we needed an approximately 21:1 speed reduction (torque multiplication) to achieve the desired output torque with a 26 mm diameter drive sprocket. Corresponding travel speed under light loading would be about 75 cm/s, ample for our applications.

The selected motor was 18 mm in length, so some creativity was needed to achieve the 21:1 speed reduction in less than 7 mm of axial space. We settled on a planetary-traction drive (Figs. 7 and 8) that enabled the large speed change in a single stage, as opposed to the two or three stages that planetary

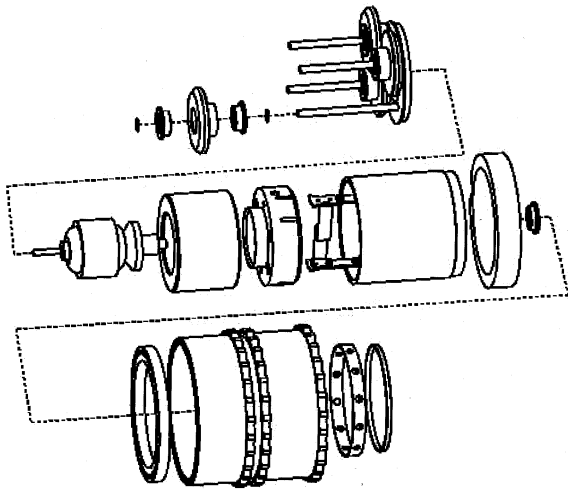


Fig. 7. Assembly diagram of the planetary-traction drive mechanism, showing the rollers, bearings and shafts (top row), motor/brush assembly (middle), and drive sprocket with encoder ring and ball bearings (bottom).

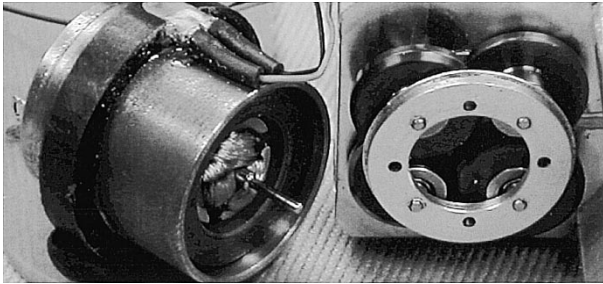


Fig. 8. Partially disassembled planetary-traction drive.

gearing would have required. The motor shaft was replaced with a hardened steel shaft ground to a pinion diameter of 0.9 mm. This drove two overlapping pairs of hard steel rollers inside a flexible cup of 22 mm inside diameter, giving a drive ratio of 25:1. The flexible cup, machined from polycarbonate, provided radial pressure to load the traction surfaces and served as the drive sprocket for the track. Achieving adequate pressure for traction without overloading the motor was tricky, requiring repeated testing and adjustment of cup stiffness, as well as precise control of part diameters and cup wall thickness. Also, radial play was designed into the rollers to allow them to balance the forces between one another without being unduly constrained by their bearings. The planetary drive supports the inboard end of each sprocket, while a thin, custom ball bearing—12 1-mm balls in a plastic cage—supports the outboard end with minimal running friction.

### C. Coupler

The function of the coupler (Figs. 9 and 10) is to securely lock adjacent Millibot modules together in train mode, while allowing easy engagement and disengagement on command. As with the other subsystems, strength and compactness were critical for the coupler. The device needed to fit between the tracks and sweep out minimal volume in the central cavity (electronics area) with changing joint angles.

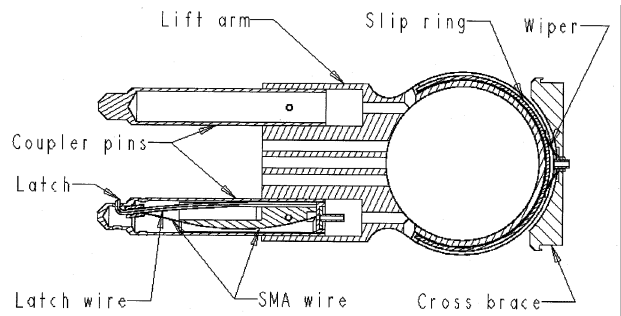


Fig. 9. Cross-sectional view of the coupler used to link together the modules.

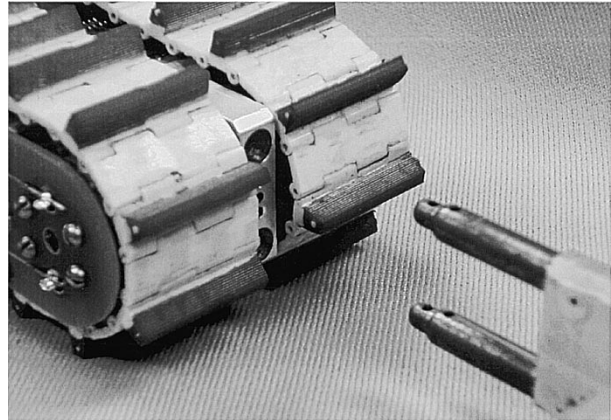


Fig. 10. Millibot uses its coupler to link together with another unit.

The design is based on a pair of hard steel pins that register with a matching receptacle to constrain five degrees-of-freedom (DOF). The *latch wire*, shaped from 0.5-mm diameter music wire, protrudes from the side of one pin to automatically lock the coupler into the receptacle after two modules have driven together. Precise parallelism between the two coupler pins and between the two mating socket holes, plus slight free play (0.03 mm) in the fit permits free insertion and retraction of the pins.

A 150- $\mu\text{m}$  shape-memory-alloy (SMA) wire (Flexinol 150HT) retracts the latch for disengagement when activated with a heating current of about 0.5 A for one second under microprocessor control. SMA actuators, although far from efficient ( $< 10\%$ ), were selected because of their exceptional specific energy: about  $10 \text{ J/cm}^3$ , an order of magnitude better than solenoids or other conventional actuators [29]. To accommodate the  $180^\circ$  rotation of the joint, a small brass slip-ring and wiper provide the power connection from the driving circuit in the central electronics cavity through the SMA wire to the grounded latch wire.

### D. Lifter

The lifting mechanism of the robot presented the toughest design challenge of any system on the vehicle. Our goal of lifting three attached modules required a torque of  $1.1 \text{ N} \cdot \text{m}$  and our available space was only 2-cm diameter by 5-cm long (the space inside the two idler sprockets). The mechanism had to be non-backdrivable under normal loads in order to hold its position, yet protected against damage in case of torque overloads due to falls, mishandling, etc. Actuation speed was not a concern since

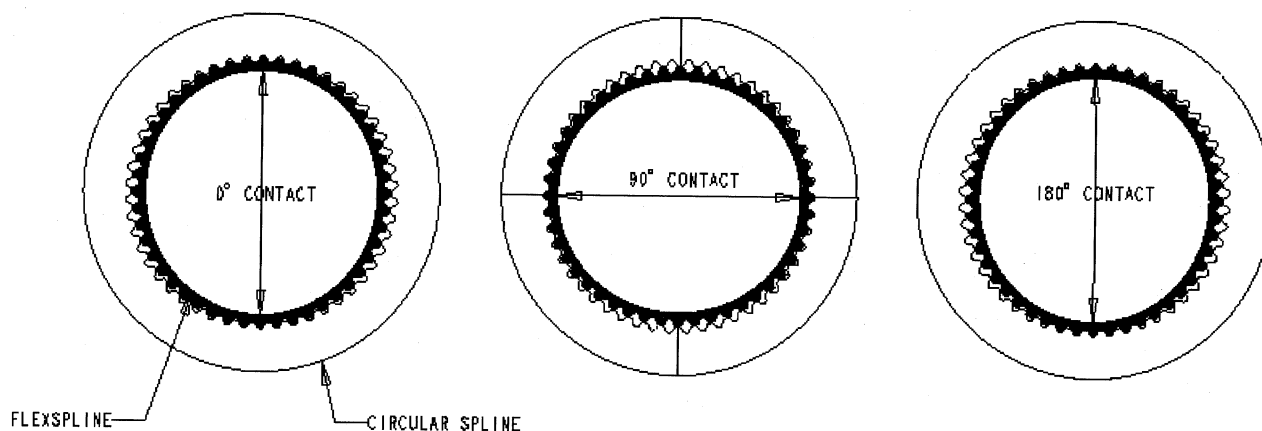


Fig. 11. Operation of a harmonic drive. An externally-toothed *flexspline* is deformed to engage the *circular spline*, which has two additional teeth. As the contact point rotates, the flexspline shifts position. By the time the contact has moved 180°, the flexspline has rotated by one tooth.

the lifter would normally be adjusted while the train was stationary, but operating efficiency was important in order to yield a reasonable battery life.

We began the design by searching for an inexpensive, high-torque motor that fit in the allowable space and chose a Mabuchi RF-130CH permanent magnet dc motor. This unit generates a continuous torque of 2 mN · m at a speed of 5000 RPM, drawing 0.5 A. Thus, a torque increase of 920:1 was required for 1.1 N·m output torque, assuming 60% efficiency. Planetary gear reduction was considered but rejected because it would have required at least four stages including a large final stage for the high torque.

Harmonic drives are a compact alternative frequently used for high-ratio, high-torque applications. The operating principle (Fig. 11) exploits a difference in the tooth count (for example, 202 versus 200) between the *circular spline* and the *flexspline* to achieve reduction ratios on the order of 100:1 in a single stage. Output torque capacity is high because of the large tooth-engagement area compared to spur gears of comparable size. Even with a 100:1 harmonic drive, however, we were still well short of meeting our overall torque goal. For additional speed reduction, we replaced the wave generator in the harmonic drive with a planetary roller assembly, similar to that for the drive mechanism. The roller drive gave us an additional 20:1 ratio, yielding an overall ratio of 2000:1 in a very compact package.

In adapting the planetary roller design for use in the harmonic drive we used a single pair of rollers, substantially widening the rollers to provide a larger contact patch. Crowning the rollers helped them to run true without damaging the inside of the flexspline. To keep the roller forces balanced on the motor shaft we designed specially-shaped shafts to allow radial play in the rollers, but still keep them diametrically opposed.

To further save space we redesigned a commercially-available harmonic drive to use a flexspline sized to just fit around our motor (Figs. 12 and 13). We cut away most of the motor housing, leaving just enough to provide the flux return path for the magnet and designed a brush holder that doubles as the means of securing the flexspline to the body.

In our design the flexspline is held fixed and the rotational output is taken from the circular spline, which transfers power through a high-friction clutch disk to a separate output ring.

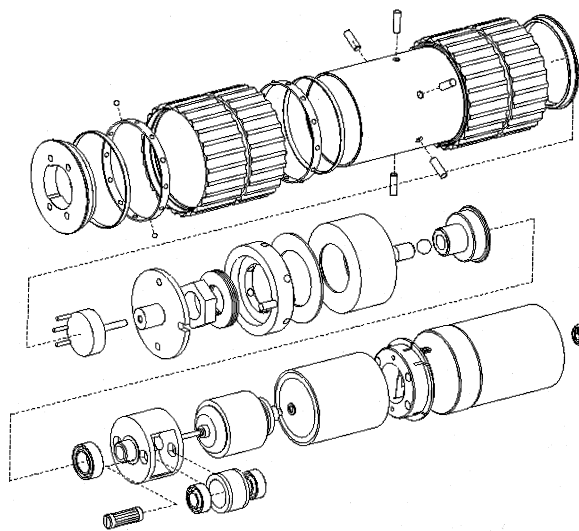


Fig. 12. Assembly diagram of the planetary harmonic lifter mechanism, showing the planetary rollers, motor/brush assembly and flexspline (bottom row), potentiometer, overload clutch and spline ring (middle) and tubular housing with external idler sprockets and ball bearings (top).

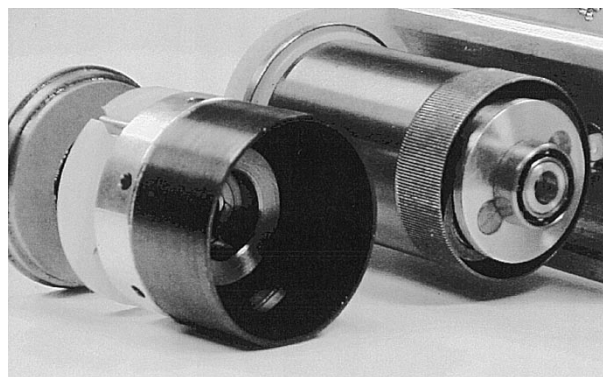


Fig. 13. Partially disassembled harmonic lifter mechanism, showing the slip clutch and circular spline on the left and the flexspline with planetary rollers on the right. The motor is located inside the flexspline.

By setting the clutch pressure, applied by three Belleville disk springs, to allow slippage at torques above 1.1 N · m, we can

utilize the full strength of the mechanism during normal operation but still protect it against excessive back-driving forces in the case of accidental abuse. A potentiometer on the output ring measures the actual lift-arm position regardless of clutch slip. Outside the tubular housing the track idler sprockets roll freely on a pair of custom integrated ball bearings, similar to those on the drive sprockets.

To form 200 teeth on a flexspline with a 19.1-mm outer diameter (OD) we had to cut uniform teeth that were just 0.132-mm (0.0052") high. We turned a blank on a lathe, mounted it on the fourth axis of a CNC milling machine and cut the teeth using a 60° carbide cutting insert mounted on a stationary arm fixed to the  $z$  axis slide. We wrote a program to compensate for the inevitable runout of the reclamped workpiece by moving the cutting tool slightly in the  $Y$  and  $Z$  directions to "follow" the profile of the workpiece as it indexed from tooth to tooth. Tooth profiles were adjusted by several degrees to compensate for curvature and flexing in operation. A similar procedure was used for machining the internal teeth of the circular spline.

We experimented with various metals for the harmonic drive splines, seeking a steel alloy with good machinability, strength and resistance to wear. A free-machining steel (12L14) was used initially, but found to be too soft and prone to wear and galling (microscopic welding between contacting faces). A number of stainless alloys were tested, but most of them were difficult to machine. Eventually we settled on 17-4PH precipitation-hardening stainless steel which is relatively hard, but machines nicely with minimal burring. This material can be heat-treated without significant distortion to  $R_{C45}$  for good strength and wear resistance. The 17-4PH performed well in gall testing of samples under heavy pressure, simulating the expected contact stresses between the splines. Testing also led to the selection of a lubricant (lead-based anti-seize compound) to minimize wear. The 17-4PH stainless has proven to be well-suited to many other parts of the Millibot Train (such as the planetary rollers) where high stress and wear are problems.

Measuring the spline teeth was critical for accurate machining and satisfactory operation, but difficult with conventional tools. The individual teeth are small enough (just 0.086 mm (.0034") wide at the top) that they can only be clearly seen with the aid of a loupe or microscope. We tried using a video microscope to measure the ratio of tooth flats to tooth gaps in order to calculate the cut depth, but resolution limitations, lighting challenges and the difficulty in identifying the true tooth edges made this procedure awkward and less accurate than needed. We finally developed a set of measuring tools consisting of three 0.15 mm (.006") diameter wires held by a fixture to lie flat in three tooth grooves evenly spaced around the circumference and a set of sized gauges (pins for the circular splines, rings for the flexspline) to test-fit between/around the wires. This method was straightforward, repeatable and gave a true measure of the effective diameter based on the tooth walls, without being affected by the shape or size of the tooth flats.

Manufacturing of the harmonic drives is very tedious, but we have successfully made several complete units and more are in process with the techniques developed. One complete unit has been run for 50 hours of continuous operation at moderate load and has produced measured output torque of 1.18 N · m at

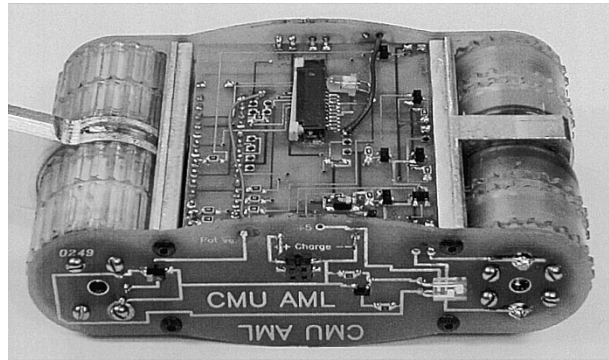


Fig. 14. Millibot Train unit with the tracks and cover removed, showing the structural printed-circuit board side plates, the aluminum cross braces and the central cavity filled with batteries, a processor board and a wireless modem.

280 mA, exceeding our target value. At the maximum measured output, efficiency was approximately 35%. The true torque limit may be somewhat higher, but we have not yet tested a unit to the point of failure.

## VI. ELECTRICAL SYSTEMS

Challenges for the Millibot Train electrical control system were similar to those for the original Millibots, but amplified because of the space taken by additional mechanical equipment. The space inside the robot (Fig. 14) is only 2.3 cm × 4.5 cm × 5 cm, which is occupied by batteries, a custom control board and an off-the-shelf radio modem. Wherever possible, surface-mount components were used to minimize the size of the control board and tall components were placed to nest with nearby objects.

### A. Power and Drive Systems

The power for the Millibot Train robot is provided by six-2/3 AAA rechargeable NiMH batteries with a voltage of 7.5-V nominal, 8.5-V fully charged, and a 290 mA/h rating. The motors are powered using H-bridges formed with surface mount hexfets and driven with PWM signals. Power consumption varies depending on how heavily the drive motors and latch mechanism are used. The batteries typically last from 15 min–1 h on a single charge.

Motor position and velocity feedback are needed for precise, coordinated control of the two drive motors in the presence of friction and voltage fluctuations. Since the motors were not available with encoders, we integrated a simple, single-channel optical encoder (phototransistor) into each side plate, receiving pulsed signals from an IRED shining through 50 holes in the drive sprocket. This yields position resolution of 0.8 mm.

### B. Communication and Control

Due to processor constraints, the Millibot modules are currently controlled off-board with a joystick. The robot has an on-board PIC processor which receives motor commands from the radio modem and controls two drive motors, one lift motor and the latch release mechanism. Communication is achieved using a spread spectrum 900-MHz radio modem from Adcon technologies and follows the IrDA link layer protocol to ensure that all information is received properly. The user can control

either a specific module or the entire train of robots at the same time. This permits maneuvering individual robots into a train configuration and then controlling the whole train in order to surmount larger obstacles or climb stairs.

There are a number of control issues that will need to be addressed to make the Millibot Train an effective vehicle. With regard to the train as a whole, we need to consider negotiating obstacles, locomoting on moderately rough terrains and recovering from nonmobile postures. Crossing steps and ditches has been discussed earlier, but it should be added that such obstacles need to be perceived either by a human driver/supervisor, or by specialized sensors such as vision or proximity sensors. For moderate terrain, a simple rearward-traveling wave, approximately matched to the track speed, should provide good mobility on many terrains, even stairs. The wavelength might be adjusted to fit the character of the terrain. Beyond this, localized sensing on the modules—contact, drive torque, proximity, etc.—could provide local information to aid in choosing a configuration.

The likelihood of falling sideways may be high especially on rough ground and when the center-of-mass of the train is high, as in climbing. The modules were purposely designed wide and low to minimize the probability of rolling onto the side and becoming stuck there. Given the number of actuators in the system, there are numerous potential strategies for recovery. For example, the train can be put into a straight configuration, then the tracks driven and/or end modules articulated to perturb the train to get it to fall back onto a driving face. We may find that there are standard motion sequences that will bring the system to the desired state in most conditions. As a last resort, one module might decouple itself so it could push the train over on one face or the other.

The other critical control task will be docking between the modules. Experiments have shown that simple LEDs and photodetectors can be used to guide the motion of one Millibot to drive into another. Such emitters and detectors could be integrated into the coupling devices at the ends of the robots. Roll alignment may be a problem on rough terrain, but it should be possible by moving both units involved in the docking to achieve substantially equal, if not level, orientations that would allow docking. There is much interesting experimental work to be done.

## VII. CHASSIS, HARDWARE INTEGRATION

The main structure of a module includes the fiberglass side plates and two aluminum cross braces (Fig. 14). Printed circuit boards serve as side plates with traces for the three motors and joint-angle potentiometer and components for the optical encoders. The track-drive sprocket assemblies mount between the side plates and the T-protrusion of the front cross brace, which also forms the coupler receptacle. Batteries and electronics fill the central cavity. Thin (0.5 mm) fiberglass sheets are bent into place to form top and bottom covers and provide smooth surfaces to support the tracks.

Several modules have been built and all functions have been successfully tested. The overall size of each module is 4.1 cm  $\times$  6.4 cm  $\times$  10.9 cm and the module center distance is 14.0 cm.

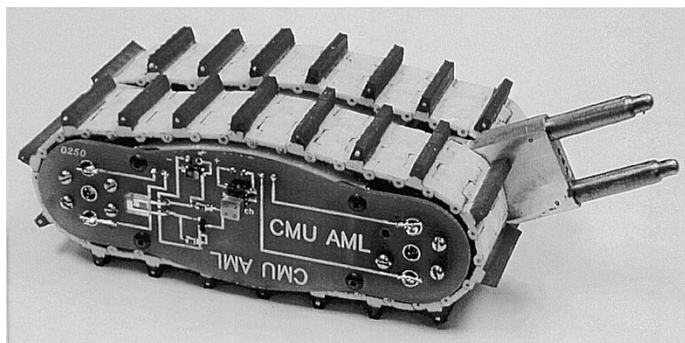


Fig. 15. Completed Millibot Train unit.

Module mass is 266 g. The size and mass of each unit significantly exceed our target specifications and the original drive and lifting performance specifications cannot be explicitly met. The increased module length mitigates this, however, permitting six modules to marginally span two full steps. This reduction in the number of modules and the greater-than-specified drive ratio (25:1 versus 21:1) offset the increased module weight, so the required drive motor torque remains virtually unchanged. With regard to lifting, a refined calculation with the lift center located coaxially with the rear sprocket (instead of the midpoint between modules) shows that cantilever lifting of three modules will require 1.14 N  $\cdot$  m of torque, just at the edge of our bench test results. Furthermore, progressive lifting and careful manipulation of joint angles to minimize actuator torque, should enable raising four modules to a vertical pose, assuming balance can be maintained.

## VIII. SUMMARY

The project goal was to build a set of Millibot modules that could be linked into a train to negotiate difficult terrains, in particular standard staircases. The concept included powered, single-axis joints that could lift three or more modules. A first prototype with adjustable joints verified that the train could handle significant obstacles, including vertical steps approximately half its length. Toward the goal of a fully functional Millibot Train robot, we identified and solved four major technical problems:

- 1) tracks that provided good traction with minimal consumption of motor power and occupied minimal volume;
- 2) track-drive actuators that provided the torque and efficiency needed for climbing steep grades (including standard staircases) and that fit into a compact package;
- 3) a coupling mechanism that joins the modules securely in a train configuration, but allows them to easily engage or disengage on command;
- 4) a compact lift mechanism capable of cantilever-lifting three modules through a range of 180°, or additional modules through progressive lifting.

Several modules have been built (Fig. 15) and all subsystems tested. Completion of six modules is imminent and will permit testing of the complete train.

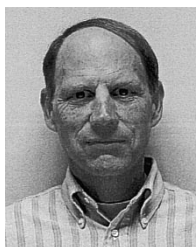
Along the way we have learned much about the design and fabrication of miniature electromechanical systems. Friction



is a critical factor at this scale and can overburden actuators if not carefully considered in the design process. Parts for centimeter-size robots are small, machining tolerances are tight (typically 0.01 mm), and a microscope and specialized measuring techniques are necessary for this work. Manufacturing costs tend to be high at this scale; the use of CNC and rapid-prototyping machines can greatly facilitate fabrication, especially when making several identical units.

## REFERENCES

- [1] R. Arkin and T. Balch, *Cooperative Multiagent Robotic Systems AI-Based Mobile Robots: Case Studies of Successful Robot Systems*, D. Kortenkamp, R. Bonasso, and R. Murphy, Eds. Cambridge, MA: MIT Press, 1998.
- [2] M. Mataric, "Issues and approaches in the design of collective autonomous agents," *Robot. Autonomous Syst.*, vol. 16, no. 2-4, pp. 321-331, Dec. 1995.
- [3] L. Parker, "Heterogeneous multi-robot cooperation," Ph.D. dissertation, Mass. Inst. Technol., Cambridge, 1994.
- [4] D. Rus, B. Donald, and J. Jennings, "Moving furniture with teams of autonomous mobile robots," presented at the *Proc. IEEE/Robotics Society of Japan Int. Workshop Intelligent Robots and Systems (IROS)*, Pittsburgh, PA, 1995.
- [5] R. Grabowski, L. Navarro-Serment, C. Paredis, and P. Khosla, "Heterogeneous teams of modular robots for mapping and exploration," *Autonomous Robot. (Special Issue on Heterogeneous and Distributed Robot.)*, vol. 8, no. 3, pp. 293-308, 2000.
- [6] L. Navarro-Serment, R. Grabowski, C. Paredis, and P. Khosla, "Modularity in small distributed robots," in *Proc. SPIE Conf. Sensor Fusion and Decentralized Control in Robotic Systems II*, vol. 3839, Sept. 1999, pp. 297-306.
- [7] G. Chirikjian and J. Burdick, "A hyper-redundant manipulator," *IEEE Robot. Automat. Mag.*, pp. 22-29, Dec. 1994.
- [8] C. Ünsal, H. Kiliççöte, and P. Khosla, "Mechatronic design of a modular self-reconfiguring robotic system," in *Proc. IEEE Int. Conf. Robotics and Automation*, 2000, pp. 1742-1747.
- [9] M. Yim, D. Duff, and K. Roufas, "PolyBot: A modular reconfigurable robot," in *IEEE Intl. Conf. Robotics and Automation*, 2000, pp. 514-520.
- [10] A. Castano, W. M. Shen, and P. Will, "CONRO: Toward deployable robots with inter-robot metamorphic capabilities," *Autonomous Robot.*, vol. 8, no. 3, pp. 309-324, 2000.
- [11] G. Homsy, A. Allen, and G. Pratt, "The Recti-Blob: A Conformal Shape-Changing Robot for Robust Locomotion Over Rough Terrain," unpublished.
- [12] S. H. Murata, H. Kurokawa, E. Yoshida, K. Tomita, and S. Kokaji, "A 3-D self-reconfigurable structure," in *Proc. IEEE Int. Conf. Robotics and Automation*, 1998, pp. 432-439.
- [13] K. Kotay, D. Rus, M. Vona, and C. McGray, "The self-reconfiguring robotic molecule," in *Proc. IEEE Int. Conf. Robotics and Automation*, Leuven, Belgium, 1998, pp. 843-851.
- [14] H. Ohno and S. Hirose, "Design of slim slime robot and its gait of locomotion," in *Proc. IEEE/RSJ Int. Conf. Intelligent Robots Systems*, vol. 2, Maui, HI, 2001, pp. 707-715.
- [15] "Orochi 12DOF Snake Like Robot," NEC Corporation, Melville, NY, 1996.
- [16] K. Dowling, "Limbless locomotion: learning to crawl with a snake robot," Ph.D. dissertation, Carnegie Mellon Univ., Pittsburgh, PA, 1997.
- [17] M. Nilsson, "Why snake robots need torsion-free joints and how to design them," in *Proc. IEEE Int. Conf. Robotics and Automation (ICRA)*, vol. 1, Leuven, Belgium, May 1998, pp. 412-417.
- [18] G. Miller, "Snake robots for search and rescue, neurotechnology for biomimetic robots," in *Proc. Int. Conf. Robotics and Automation (ICRA)*, Leuven, Belgium, May 16-21, 1998, pp. 412-417.
- [19] S. Hirose, Xevius Stair-Climbing Robot. [Online]. Available: <http://mozu.mes.titech.ac.jp/research/mobile/NewCrawler/crawler.html>
- [20] H. Schempf, E. Mutschler, C. Piepgras, J. Warwick, B. Chemel, S. Boehmke, W. Crowley, R. Fuchs, and J. Guyot, "Pandora: Autonomous urban reconnaissance system," in *Proc. IEEE Int. Conf. Robotics and Automation*, vol. 3, Detroit, MI, May 1999, pp. 2315-2321.
- [21] "Urban Robot," IS Robotics (now iRobot), Sommerville, MA, 1999.
- [22] S. Hirose, A. Morishima, S. Tukagosi, T. Tsumaki, and H. Monobe, "Design of practical snake vehicle: Articulated body mobile robot KR-II," in *Proc. 5th Int. Conf. Advanced Robotics*, Pisa, Italy, 1991, pp. 833-838.
- [23] S. Hirose, Souryu. [Online]. Available: <http://mozu.mes.titech.ac.jp/research/snake/soryu/index.html>
- [24] S. Hirose, T. Shirasu, and E. Fukushima, "Proposal for cooperative robot 'Gunryu' composed of autonomous segments," *Robot. Autonomous Syst.*, vol. 17, pp. 107-118, 1996.
- [25] S. Ridgeway, P. Adsit, and C. Crane, "Development of an articulated transporter/manipulator system," *Invited Paper for Special Issue on Highly Redundant Manipulators of Advanced Robotics*, *Trans. Robot. Soc. Jpn.*, vol. 9, no. 3, pp. 301-316, 1995.
- [26] M. Bekker, *Theory of Land Locomotion: The Mechanics of Vehicle Mobility*. Ann Arbor, MI: Univ. Mich. Press, 1956, pp. 379-390.
- [27] ———, *Theory of Land Locomotion: The Mechanics of Vehicle Mobility*. Ann Arbor, MI: Univ. Mich. Press, 1956, p. 335.
- [28] C. Bererton and P. Khosla, "Toward a team of robots with repair capabilities: Docking systems," in *Proc. IEEE Int. Conf. Robotics Animation*, vol. 3, Honolulu, HI, 2001, pp. 2923-2928.
- [29] TiNi Alloy Company, San Leandro, CA. [Online]. Available: <http://www.sma-mems.com/>



**H. Benjamin Brown, Jr.** received the B.S. and M.S. degrees in mechanical engineering from Carnegie Mellon University, Pittsburgh, PA, in 1967 and 1976, respectively.

After 12 years in various industry research and development and design-related positions, he joined the Robotics Institute, Carnegie Mellon University, in 1981 and began working on dynamically stabilized, legged, running robots. He was primarily responsible for the mechanical design of four running robots of unequalled performance. Currently, he is a Project Scientist at the Robotics Institute. He holds one patent with two pending and has authored or coauthored approximately 40 conference and journal papers, mainly in the field of mobile robotics. His current research projects include the design and development of three-dimensional snake robots, "millibot" trains for enhanced mobility, and highly efficient, dynamic hopping and running robots. His research interests include the analysis, design and control of robots and electromechanical systems and specializes in the development of high-performance structures and equipment and dynamically stabilized robots.

Mr. Brown's "Gyrover" gyroscopically stabilized, single-wheel robot was one of five robotics finalists in the 1998 *Discover Magazine* Technology Awards.



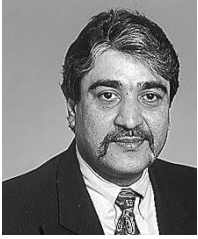
**J. Michael Vande Weghe** received the S.B.E.E. degree from the Massachusetts Institute of Technology, Cambridge, in 1990 and the M.S. degree in robotics from Carnegie Mellon University (CMU), Pittsburgh, PA, in 2002.

From 1990 to 1998, he worked in industry in the areas of power electronics, computer speech recognition, and voice-routing of telephone calls. In 1998, he was a Research Programmer at the Institute for Complex Engineered Systems, CMU, where he worked on distributed information security systems, multiagent planning algorithms, and the mechanical design of miniature autonomous surveillance robots. Currently, he is at the Neurobotics Laboratory, Robotics Institute, CMU, where he is building an anatomically correct mechanical model of the human hand.



**Curt A. Bererton** received the B.S. degree in computer engineering from the University of Alberta, Edmonton, AB, Canada, in 1998 and the M.S. degree in robotics from Carnegie Mellon University (CMU), Pittsburgh, PA, in 2000. He is currently working toward the Ph.D. degree in robotics at CMU.

His main research interest is in self-sustaining robot ecologies. Toward this goal, he has studied the utility of modular robots, repairable robots, fault tolerance, and probabilistic planning for cooperative teams of robots.



**Pradeep K. Khosla** (S'83–M'83–SM91–F'95) received the B.Tech. degree (Hons.) from the Indian Institute of Technology (IIT), Kharagpur, India, in 1980 and the M.S. and Ph.D. degrees from Carnegie Mellon University (CMU), Pittsburgh, PA, in 1984 and 1986, respectively.

From 1986 to 1990, he was an Assistant Professor of electrical and computer engineering and robotics at CMU where, from 1990 to 1994, he was an Associate Professor and, in 1994, he became a Full Professor.

From January 1994 to August 1996, he was on leave from CMU and served as a Defense Advanced Research Projects Agency (DARPA) Program Manager in the Software and Intelligent Systems Technology Office (SISTO), Defense Sciences Office (DSO), and Tactical Technology Office (TTO), Arlington, VA, where he managed advanced research and development programs. From January 1997 to June 1999, he was the Founding Director of the Institute for Complex Engineered Systems, CMU. Since July 1999, he has been the Head of the Electrical and Computer Engineering Department at CMU where he is currently the Philip and Marsha Dowd Professor of Engineering and Robotics. His research interests are in the areas of internet-enabled distributed and collaborative design, collaborating autonomous systems, agent-based architectures for embedded control, software composition and reconfigurable software for real-time embedded systems, reconfigurable and distributed robotic systems, distributed information systems and intelligent instruments for biomedical applications. His research is multidisciplinary and has focused on the theme of “creating complex embedded systems and information systems through composition of and collaboration amongst building blocks.”